Manuscript

Click here to view linked References

Click here to download Manuscript FhCaBPstrucpaper-revised.docx

SHORT COMMUNICATION

Fasciola hepatica calcium binding protein FhCaBP2: Structure of the dynein light chain-like domain

Thanh H. Nguyen[1,2], Charlotte M. Thomas[3,4], David J. Timson[3,5] and Mark J. van Raaij[1]

[1]Dpto de Estructura de Macromoleculas, Centro Nacional de Biotecnologia - CSIC, calle Darwin 3, E-28049 Madrid, Spain.

[2]Genetic Engineering Laboratory, Institute of Biotechnology (IBT-VAST), 18 Hoang Quoc Viet, Cau Giay, Hanoi, Vietnam.

[3]School of Biological Sciences, Queen's University Belfast, Medical Biology Centre, 97 Lisburn Road, Belfast, BT9 7BL, UK.

[4]Institute for Global Food Security, Queen’s University Belfast, 18-30 Malone Road, Belfast, BT9 5BN, UK.

[5]School of Pharmacy and Biomolecular Sciences, University of Brighton, Huxley Building, Lewes Road Brighton BN2 4GJ, UK.

Running title: FhCaBP2 structure

Acknowledgements Crystallographic data was collected at beamline XALOC-BL13 at ALBA Synchrotron Light Facility with the collaboration of Fernando Gil and Jordi Juanhuix. MJvR thanks the Spanish Ministry of Economy and Competitiveness for grants BFU2011-24843 and BFU2014-53425-P. THN received a PhD fellowship from the Consejo Superior de Investigaciones Científicas and Vietnam Academy of Science and Technology. CMT is in receipt of a PhD studentship from the Department of Employment and Learning, Northern Ireland (DELNI, UK).

Abstract The common liver fluke *Fasciola hepatica* causes an increasing burden on human and animal health, partly because of the spread of drug resistant isolates. As a consequence there is considerable interest in developing new drugs to combat liver fluke infections. A group of potential targets is a family of calcium binding proteins which combine an N-terminal domain with two EF-hand motifs and a C-terminal domain with predicted similarity to dynein light chains (DLC-like domain). The function of these proteins is unknown, although in several species they have been localised to the tegument, an important structure at the host-parasite interface. Here, we report the x-ray crystal structure of the DLC-like domain of FhCaBP2 (*Fasciola hepatica* calcium binding protein 2), solved using single-wavelength anomalous diffraction and refined at 2.3 Å resolution in two different crystal forms. The FhCaBP2 DLC-like domain has a structure similar to other DLC domains, with an anti-parallel β-sheet packed against an α-helical hairpin. Like other DLC domains, it dimerizes through its β_2-strand, which extends in an arch and forms the fifth strand in an extended β-sheet of the other monomer. The structure provides molecular details of the dimerization of FhCaBP2, the first example from this family of parasite proteins.

Keywords Liver fluke · Calcium-Binding Protein · Dynein Light Chain · Crystal Structure · Helminth Protein

Introduction

Parasitic infections from worms of the class Trematoda are causing an increasing burden on human and animal health. For example, it is estimated that several million humans are infected with the common liver fluke *Fasciola hepatica* – and this zoonotic infection is classed by WHO as a neglected tropical disease (Robinson and Dalton 2009). Globally, the impact of *F. hepatica* infections of farm animals is estimated to result in several billions of dollars of agricultural losses per annum (Boray 1994; Schweizer et al. 2005). This increasing burden results partly because of the spread of drug resistant isolates of liver flukes. Resistance to triclabendazole, a generally safe and effective treatment for liver fluke infections, is now widespread in flukes which infect farm animals and the first incidences of humans infected with resistant flukes has also been reported (Cabada et al. 2016; Gil et al. 2014; Winkelhagen et al. 2012). As a consequence, there is considerable interest in developing new drugs to combat liver fluke, and other trematode, infections. Much of this interest focuses on the identification of possible novel targets from these organisms. Proteins which are unique to trematodes, and not present in the host, are particularly attractive, since antagonism of these molecules is less likely to have detrimental effects on the host.

One such group of potential targets is a family of calcium binding proteins which combine an N-terminal domain with two EF-hand motifs and a C-terminal domain with predicted similarity to dynein light chains (DLC-like domain) (Russell and Timson 2014; Thomas and Timson 2016). This combination of domains is unique: no mammalian proteins with EF-hand and DLC-like domains in the same protein are known. The function of these proteins is unknown, and it is not known if the proteins are essential for infection or survival of the parasite (knock-out or RNAi studies on these proteins have not been reported). One family member (SmTAL3/Sm20.8 from *Schistosoma mansoni*) has been shown to form part of a high molecular mass protein complex together with dynein light chain; therefore, it has been postulated that its role may be to link calcium signalling with microtubule regulation (Hoffmann and Strand 1997). However, it should be noted that SmTAL3 does not bind calcium ions, although other family members do (Thomas et al. 2015). In several species the family members have been localised to the tegument, suggesting a potential role in the regulation of this important structure at the host-parasite interface (Havercroft et al. 1990; Huang et al. 2007; Jeffs et al. 1991; Kim et al. 2012; Mohamed et al. 1998; Subpipattana et al. 2012; Vichasri-Grams et al. 2006; Xu et al. 2014; Zhang et al. 2012). In *Schistosoma spp*, there are typically large numbers of different family members expressed. For example, *S. mansoni* has at least 13 different members and several of these have been shown to illicit allergen-like IgE immune responses (Fitzsimmons et al. 2012). Consequently, these proteins are also

considered as possible vaccines as well as drug targets (Fitzsimmons et al. 2007; Fitzsimmons et al. 2004; Zhang et al. 2012). In *F. hepatica*, there are at least four family members (FH22, FhCaBP2, FhCaBP3 and FhCaBP4), with distinct biochemical properties (Banford et al. 2013; Orr et al. 2012; Ruiz de Eguino et al. 1999; Thomas and Timson 2015). Similarly, the *S. mansoni* tegumental allergen (TAL) proteins that have been characterised biochemically show different drug and ion binding properties (Thomas et al. 2015). This suggests that each protein may have a subtly different function in the organism (Russell and Timson 2014; Thomas and Timson 2016).

A major barrier in understanding the biology of these proteins and in their possible development as vaccines or as drug targets is a lack of experimental, high-resolution structural data. To date, a number of molecular models have been reported but, like all models, these are highly reliant on the template structures (Banford et al. 2013; Orr et al. 2012; Thomas et al. 2015; Thomas and Timson 2015). Crystallization, but not structure solution, of the DLC-like domain of *S. mansoni* TAL2 (SmTAL2, Sm21.7) has also been reported (Costa et al. 2014). Here, we report the crystallographic structure of the DLC-like domain of FhCaBP2 (UniProt: A0A0B5GUS3).

Materials and Methods

Purification and crystallisation of FhCaBP2

Recombinant hexahistidine-tagged FhCaBP2 was expressed in *Escherichia coli* HMS174(DE3) and initial purification carried out using cobalt affinity resin as previously described (Thomas and Timson 2015). Further purification was conducted by anion-exchange chromatography (Resource Q6 column, GE-Healthcare Biosciences, Uppsala, Sweden), after dialysing the protein against 10 mM Tris-HCl pH 8.5, 1 mM dithiothreitol. The protein was eluted in the same buffer with a linear gradient of 0-0.65 M sodium chloride, and eluted in two adjacent peaks around 0.3 M. It is not clear what the difference is between the two peaks, because on SDS-PAGE the same band is observed. Fractions containing pure protein from each peak were pooled separately and concentrated up to 16 mg/ml using an Amicon Ultra concentrator with a molecular weight cut-off of 10 kDa (Millipore, Billerica MA, USA). Three washes with 10 ml of 10 mM Tris-HCl pH 8.5, 50 mM sodium chloride were applied. The samples were stored at 4 °C prior to crystallization trials.

FhCaBP2 protein was crystallized using the sitting drop vapour diffusion method (MRC 2-well Swissci crystallization plates, Molecular Dimensions, Newmarket, UK), adding 50 µl of precipitant solution to the reservoir wells. To form the drops, protein solution (0.2 µl) was mixed with 0.2 µl of the respective reservoir

solution (Genesis RSP 150 workstation; Tecan, Männedorf, Switzerland). Plates were incubated at 21 ºC. After two months of incubation, a crystal was obtained in each of two drops, one in the presence of 20 % (w/v) PEG 3350 and 0.2 M sodium tartrate and one with the same precipitant and 0.2 M potassium citrate. To generate the heavy atom derivative crystal, a few grains of solid methylmercury chloride were added to the reservoir of a crystal grown in the presence of sodium tartrate. The drop was equilibrated overnight with the reservoir and 2 μl of reservoir solution were then added to the drop and incubated for about 5 min. The native crystal and derivative crystal were harvested with a Litholoop (Molecular Dimensions, Newmarket, UK) and flash-cooled in liquid nitrogen without cryo-protection.

Six-histidine-tagged recombinant C-terminal domain (residues 99-189) was also expressed in *E. coli* as previously described (Thomas and Timson 2015). It was purified using the same protocol as described above for the full-length protein, in this case a single peak was observed after anion exchange chromatography, eluting at around 0.15 M sodium chloride. Crystallization of C-terminal domain protein was performed in the same manner as for the full-length protein, crystals were obtained within two weeks from the condition containing 20 % (w/v) PEG 3350 and 0.2 M sodium tartrate. Crystals were harvested as above.

X-ray crystallography data collection and structure solution

Crystallographic data were collected from a methylmercury chloride derivative crystal at the BL13-XALOC beamline of the ALBA synchrotron (Juanhuix et al. 2014), using a wavelength at which significant anomalous signal from the added mercury atoms was expected (1.0056 Å). Crystallographic data were integrated using MOSFLM (Battye et al. 2011) and further processed using POINTLESS, SCALA and TRUNCATE (Evans 2011) from the CCP4-suite (Winn et al. 2011) to obtain structure factor amplitudes. Structure solution was done using AUTOSHARP (Vonrhein et al. 2007), which employs SHELX for heavy atom substructure determination (Sheldrick 2010), SHARP for phase determination (de La Fortelle and Bricogne 1997), SOLOMON for solvent flattening (Abrahams and Leslie 1996) and ARPWARP for automated model building (Langer et al. 2008). The auto-traced model was completed using COOT (Emsley et al. 2010) and refined using REFMAC5 (Murshudov et al. 2011) (10% of reflections were selected for calculation of Rfree (Brunger 1993)). For structure solution of the non-derivatised C-terminal domain, data was also collected at BL13-XALOC. Structure solution by molecular replacement was performed using PHASER (McCoy et al. 2007), after increasing the number of allowed C-α clashes to 20%. The model was completed using COOT and refined using REFMAC5 as before. Validation was done with MOLPROBITY (Chen et al. 2010). Structure comparisons, including r.m.s.d. and Z-

score calculations, were performed using the DALI server (Holm and Rosenstrom 2010). Figures were made using PyMol (The PyMol Molecular Graphics System, Version 1.5.0.4. Schrödinger, LLC). Protein assembly parameters were calculated using PISA (Krissinel and Henrick 2007) and the PIC server (Tina et al. 2007). Data collection, phasing and refinement parameters are shown in Table 1.

Results and Discussion

Structure of the DLC-like domain of FhCaBP2

In initial experiments, we attempted to crystallise full length FhCaBP2 (residues 1-189). This resulted in the formation of single prism-shaped crystals (Figure 1A), belonging to space group $P4_12_12$, with one protein molecule in the asymmetric unit. However, upon analysis, it became apparent that these crystals only contained the C-terminal DLC-like domain of the protein. Interestingly, a similar outcome was reported following attempts to crystallise SmTAL2 (Costa et al. 2014). This suggests that the flexible linker between the EF-hand domain and the DLC-like domain in these proteins is susceptible to degradation by proteases. Indeed, we speculate that this may be important in their normal, *in vivo* functioning. The complete absence of the EF-hand domain in the structure is interesting and may indicate that this domain is less stable to proteolysis than the DLC-like domain. Later, we also crystallized the C-terminal domain (residues 99-189) separately. In this case, crystals belonging to space group $P6_422$ were obtained, also with one protein monomer in the asymmetric unit (Figure 1B).

A methylmercury chloride derivative of a crystal of the $P4_12_12$ form was prepared and diffraction data were collected from it (Table 1). Three heavy atom sites were located, of which one was well-occupied and later modelled as a mercury ion between cysteine residues 153 and 181. Single-wavelength anomalous dispersion led to good phases, which were used in an automatic model building procedure to yield a protein model with 97 residues (Ala92 to Arg188; the entire C-terminal DLC-like domain plus a few residues of the linker between the N-terminal EF-hand domain and C-terminal DLC-like domain). Careful refinement at 2.3 Å resolution and inspection of electron density maps allowed the addition of a mercury ion, two chloride ions and 57 water molecules (PDB code 5FWZ). Using this structure, the structure of a native crystal of the $P6_422$ space group was solved by molecular replacement and refined to 2.3 Å resolution. The final model of this structure contains 89 amino acids, Ile99 to Pro187, plus nine residues of the N-terminal expression tag and eight water molecules (PDB code 5FX0). The packing of the molecules in the two crystal forms is very different, apart from the dimer interaction described below. The two structures of the DLC-domain are identical in the two crystal forms; a root

mean squared deviation (r.m.s.d) of only 0.5 Å is obtained when the C-α atoms of residues 99-187 are superposed.

The structure of the DLC-like domain revealed a compact, largely β-sheet structure (Figure 2). It consists of an anti-parallel β-sheet packed against a hairpin of α-helices (Figure 2A). The order of the β-strands is $\beta_0\beta_3\beta_4\beta_1$ and the $\alpha_1\alpha_2$ hairpin is between strands β_0 and β_1 in the primary sequence. The structure is similar to many of the DLC domains in the PDB database. They can be superimposed with an r.m.s.d. of 1.5-2.0 Å (81-85 superposed residues, DALI Z-scores between 13 and 14). Although Cys153 and Cys181 are physically close to each other, no cystine bond is observed between them. Cystine bonds are also not observed in other DLC-like domains (for example in PDB entries 1CMI, 3E2B or 4DS1 (Benison et al. 2008; Liang et al. 1999; Romes et al. 2012)). Two *cis*-peptides are observed in the structure, Ala92-Pro93 (in the putative linker between the N- and C-terminal domains) and Arg149-Val150, a non-proline cis-peptide. Non-proline cis-peptides are rare, but the observed electron density clearly indicates their presence in this case. The experimental structure is in good agreement with the DLC-like domain of the previously published molecular model (Thomas and Timson 2015); residues 99-187 can be superposed with an rmsd of 2.7 Å (Figure 3A). Significant differences are only observed for the inter-domain linker, the loop between α_1 and α_2, strand β_2 and the very C-terminal residues. The model was of a monomeric protein and so this structure enables us to understand, for the first time, the molecular basis of dimerization in these proteins.

Dimer interactions

The DLC-like domain of FhCaBP2 dimerises through an extended β-sheet structure (Figure 2). The interface is largely composed of the β_2-strand from each subunit, bent through almost 180° into an arch. Strand β_2 protrudes from the back of the molecule and interacts with strand β_1 of another monomer to form a symmetric dimer (i.e., the dimer contains β-sheets $\beta_0\beta_3\beta_4\beta_1\beta_2'$ and $\beta_0'\beta_3'\beta_4'\beta_1'\beta_2$; Figure 2B). In both crystal forms, the same crystallographic dimer is observed, with an inter-monomer interface of about 1100 $Å^2$ and an estimated dissociation energy of approximately 15 $kcal.mol^{-1}$. Key residues in the interaction are those belonging to the β_1- and β_2-strands, five main-chain hydrogen bonds hold together each of the extended β-sheets. Side-chains of residues of the same strands also contribute to the hydrophobic interaction interface. Further hydrophobic interactions are formed between residues of the β_2-strand and the α_2-helix and between opposing β_1-and β_4-strands. At least six additional hydrogen bonds involving side-chains are also present. Homo-dimer formation of the FhCaBP2 DLC-like domain is consistent with biochemical data (Thomas and Timson 2015) and identical to

known structures of DLC-like domains. This arrangement is also seen in DLC dimers from *Saccharomyces cerevisiae* (Dyn2p) (PDB 4DS1, Z-score 13.8, r.m.s.d. 1.8 Å^2 when 84 Cα atoms are aligned; Romes et al. 2012), in the rat 8 kDa DLC (PDB 1F3C; Z-score 10.3, r.m.s.d. 2.2 Å^2 when 86 Cα atoms are aligned; Fan et al. 2001) and in human dynein light chain 8 (PDB 3ZKE, Z-score 13.9, r.m.s.d. 1.6 Å^2 when 83 Cα atoms are aligned; Gallego et al. 2013), albeit with somewhat smaller interaction surfaces (around 800 Å^2) and predicted interaction energies (around 10 kcal.mol^{-1}). While the conservation of the structural scaffold means that dimer interactions are almost identical in terms of main-chain hydrogen bonds, the low sequence identity between the FhCaBP2 DLC-like domain with the DLC domains mentioned above of around 20% means side-chain electrostatic interactions, hydrogen bonds and van der Waals interactions are very different.

In *S. cerevisiae* Dyn2p, peptides from the nuclear pore component Nup159p dock into the cleft between the two monomers of the DLC, further extending the β-sheet structure (Romes et al. 2012). Peptides from neuronal nitric oxide synthase (nNOS) and BCL2-like 11 (BIM, an apoptosis regulator) both bind into the cleft between the monomers in a similar arrangement to the Dyn2p-Nup159p interaction (PDB 1F95, 1F96 (Fan et al. 2001)). In human dynein light chain 8, peptides from the Nek7 protein kinase also bind to the same site (PDB 3ZKE, 3ZKF; Gallego et al. 2013). This demonstrates that a wide variety of different binding partners can interact with DLC dimers in this manner and suggests that FhCaBP2 (and other proteins from this family) may also exploit this mode of protein-protein interaction. A superposition of the FhCaBP2 DLC-like domain with the human dynein light chain 8 - Nek7 protein kinase peptide structure (Figure 3B) shows that, although the structures generally overlap very well, the $\alpha_1\alpha_2$-loop, $\beta_1\beta_2$-loop, β_2-strand and $\beta_2\beta_3$-loop adopt somewhat different conformations (in *S. cerevisiae* Dyn2p and rat 8 kDa DLC, these secondary structure elements have a very similar conformation to that in human dynein light chain 8). In the superposition, the FhCaBP2 $\beta_2\beta_3$-loop (highlighted with an arrow in Figure 3B) overlaps with the peptide, suggesting that the FhCaBP2 DLC-like domain, if it is involved in further protein-protein interactions, may need to change conformation to bind another protein or may bind its interaction partners in a somewhat different manner.

Conclusions

The structure reported here enables us to understand the dimerization of DLC-like domains of this class of proteins and validates the modelling techniques used to predict the structure of this domain in a range of proteins. It also suggests how this family of proteins might interact with other proteins through the DLC-like domain. The *in vivo* functions of this family of proteins remain enigmatic. However, it is hypothesised that they

222 may perform roles in calcium signalling in the tegument (Thomas and Timson 2016). If such a role is
223 demonstrated then they would be very attractive targets for the development of novel anthelminthic drugs. One
224 possible strategy would be the identification of molecules which disrupt dimer formation. This structure
225 provides vital information to enable that process and the low sequence similarity in the dimerization region
226 suggests that it should be possible to identify molecules which selectively target trematode proteins without
227 affecting host DLCs.

228

229 References

230 Abrahams JP, Leslie AG (1996) Methods used in the structure determination of bovine mitochondrial F1
231 ATPase. Acta Crystallogr D Biol Crystallogr 52(Pt 1):30-42 doi:10.1107/s0907444995008754
232 Banford S, Drysdale O, Hoey EM, Trudgett A, Timson DJ (2013) FhCaBP3: A *Fasciola hepatica* calcium
233 binding protein with EF-hand and dynein light chain domains. Biochimie 95:751-758
234 doi:10.1016/j.biochi.2012.10.027; 10.1016/j.biochi.2012.10.027
235 Battye TG, Kontogiannis L, Johnson O, Powell HR, Leslie AG (2011) iMOSFLM: a new graphical interface for
236 diffraction-image processing with MOSFLM. Acta Crystallogr D Biol Crystallogr 67(Pt 4):271-81
237 doi:10.1107/s0907444910048675
238 Benison G, Karplus PA, Barbar E (2008) The interplay of ligand binding and quaternary structure in the diverse
239 interactions of dynein light chain LC8. J Mol Biol 384(4):954-66 doi:10.1016/j.jmb.2008.09.083
240 Boray JC (1994) Diseases of domestic animals caused by flukes. Food and Agricultural Organisation of the
241 United Nations, Rome
242 Brunger AT (1993) Assessment of phase accuracy by cross validation: the free R value. Methods and
243 applications. Acta Crystallogr D Biol Crystallogr 49(Pt 1):24-36 doi:10.1107/s0907444992007352
244 Cabada MM, Lopez M, Cruz M, Delgado JR, Hill V, White AC, Jr. (2016) Treatment Failure after Multiple
245 Courses of Triclabendazole among Patients with Fascioliasis in Cusco, Peru: A Case Series. PLoS Negl
246 Trop Dis 10(1):e0004361 doi:10.1371/journal.pntd.0004361
247 Chen VB, et al. (2010) MolProbity: all-atom structure validation for macromolecular crystallography. Acta
248 Crystallogr D Biol Crystallogr 66(Pt 1):12-21 doi:10.1107/s0907444909042073
249 Costa MA, Rodrigues FT, Chagas BC, Rezende CM, Goes AM, Nagem RA (2014) Preliminary crystallographic
250 studies of a *Schistosoma mansoni* antigen (Sm21.7) dynein light-chain (DLC) domain. Acta Crystallogr
251 F, Struct Biol Commun 70(Pt 6):803-807 doi:10.1107/S2053230X14009273
252 de La Fortelle E, Bricogne G (1997) Maximum-likelihood heavy-atom parameter refinement for multiple
253 isomorphous replacement and multiwavelength anomalous diffraction methods. Methods in
254 Enzymology. Volume 276. Academic Press, p 472-494
255 Emsley P, Lohkamp B, Scott WG, Cowtan K (2010) Features and development of Coot. Acta Crystallogr D
256 Biol Crystallogr 66(Pt 4):486-501 doi:10.1107/s0907444910007493
257 Evans PR (2011) An introduction to data reduction: space-group determination, scaling and intensity statistics.
258 Acta Crystallogr D Biol Crystallogr 67(Pt 4):282-92 doi:10.1107/s090744491003982x
259 Fan J, Zhang Q, Tochio H, Li M, Zhang M (2001) Structural basis of diverse sequence-dependent target
260 recognition by the 8 kDa dynein light chain. J Mol Biol 306(1):97-108 doi:10.1006/jmbi.2000.4374
261 Fitzsimmons CM, et al. (2012) The *Schistosoma mansoni* tegumental-allergen-like (TAL) protein family:
262 influence of developmental expression on human IgE responses. PLoS Negl Trop Dis 6(4):e1593
263 doi:10.1371/journal.pntd.0001593
264 Fitzsimmons CM, et al. (2007) Factors affecting human IgE and IgG responses to allergen-like *Schistosoma*
265 *mansoni* antigens: Molecular structure and patterns of in vivo exposure. Int Arch Allergy Imm
266 142(1):40-50 doi:10.1159/000095997
267 Fitzsimmons CM, Stewart TJ, Hoffmann KF, Grogan JL, Yazdanbakhsh M, Dunne DW (2004) Human IgE
268 response to the *Schistosoma haematobium* 22.6 kDa antigen. Parasite Immunol 26(8-9):371-376
269 doi:10.1111/j.0141-9838.2004.00721.x
270 Gallego P, Velazquez-Campoy A, Regue L, Roig J, Reverter D (2013) Structural analysis of the regulation of
271 the DYNLL/LC8 binding to Nek9 by phosphorylation. J Biol Chem 288(17):12283-12294
272 doi:10.1074/jbc.M113.459149

Gil LC, Diaz A, Rueda C, Martinez C, Castillo D, Apt W (2014) [Resistant human fasciolasis: report of four patients]. Rev Med Chile 142(10):1330-3 doi:10.4067/s0034-98872014001000014

Havercroft JC, Huggins MC, Dunne DW, Taylor DW (1990) Characterisation of Sm20, a 20-kilodalton calcium-binding protein of *Schistosoma mansoni*. Mol Biochem Parasitol 38(2):211-219

Hoffmann KF, Strand M (1997) Molecular characterization of a 20.8-kDa *Schistosoma mansoni* antigen. Sequence similarity to tegumental associated antigens and dynein light chains. Journal Biol Chem 272(23):14509-14515

Holm L, Rosenstrom P (2010) Dali server: conservation mapping in 3D. Nucleic Acids Res 38(Web Server issue):W545-9 doi:10.1093/nar/gkq366

Huang Y, et al. (2007) A novel tegumental protein 31.8 kDa of Clonorchis sinensis: sequence analysis, expression, and immunolocalization. Parasitol Res 102(1):77-81 doi:10.1007/s00436-007-0728-z

Jeffs SA, Hagan P, Allen R, Correa-Oliveira R, Smithers SR, Simpson AJ (1991) Molecular cloning and characterisation of the 22-kilodalton adult *Schistosoma mansoni* antigen recognised by antibodies from mice protectively vaccinated with isolated tegumental surface membranes. Mol Biochem Parasitol 46(1):159-167 doi:0166-6851(91)90209-O

Juanhuix J, et al. (2014) Developments in optics and performance at BL13-XALOC, the macromolecular crystallography beamline at the ALBA synchrotron. J Synchrotron Radiat 21(Pt 4):679-89 doi:10.1107/s160057751400825x

Kim YJ, et al. (2012) Identification and characterization of a novel 21.6-kDa tegumental protein from Clonorchis sinensis. Parasitol Res 110:2061-2066 doi:10.1007/s00436-011-2681-0

Krissinel E, Henrick K (2007) Inference of macromolecular assemblies from crystalline state. J Mol Biol 372(3):774-97 doi:10.1016/j.jmb.2007.05.022

Langer G, Cohen SX, Lamzin VS, Perrakis A (2008) Automated macromolecular model building for X-ray crystallography using ARP/wARP version 7. Nat Protoc 3(7):1171-9 doi:10.1038/nprot.2008.91

Liang J, Jaffrey SR, Guo W, Snyder SH, Clardy J (1999) Structure of the PIN/LC8 dimer with a bound peptide. Nat Struct Biol 6(8):735-740 doi:10.1038/11501

McCoy AJ, Grosse-Kunstleve RW, Adams PD, Winn MD, Storoni LC, Read RJ (2007) Phaser crystallographic software. J Appl Crystallogr 40(Pt 4):658-674 doi:10.1107/s0021889807021206

Mohamed MM, Shalaby KA, LoVerde PT, Karim AM (1998) Characterization of Sm20.8, a member of a family of schistosome tegumental antigens. Mol Biochem Parasitol 96(1-2):15-25 doi:S0166-6851(98)00088-7

Murshudov GN, et al. (2011) REFMAC5 for the refinement of macromolecular crystal structures. Acta Crystallogr D Biol Crystallogr 67(Pt 4):355-67 doi:10.1107/s0907444911001314

Orr R, et al. (2012) FhCaBP4: a *Fasciola hepatica* calcium-binding protein with EF-hand and dynein light chain domains. Parasitol Res 111(4):1707-1713 doi:10.1007/s00436-012-3010-y

Robinson MW, Dalton JP (2009) Zoonotic helminth infections with particular emphasis on fasciolosis and other trematodiases. Philos Trans R Soc B-Biol Sci 364(1530):2763-2776 doi:10.1098/rstb.2009.0089

Romes EM, Tripathy A, Slep KC (2012) Structure of a yeast Dyn2-Nup159 complex and molecular basis for dynein light chain-nuclear pore interaction. J Biol Chem 287(19):15862-73 doi:10.1074/jbc.M111.336172

Ruiz de Eguino AD, et al. (1999) Cloning and expression in *Escherichia coli* of a *Fasciola hepatica* gene encoding a calcium-binding protein. Mol Biochem Parasitol 101(1-2):13-21

Russell SL, Timson DJ (2014) Calcium binding proteins in the liver fluke, *Fasciola hepatica*. New Developments in Calcium Signaling Research. Nova Science Publishers, Inc, p 89-104

Schweizer G, Braun U, Deplazes P, Torgerson PR (2005) Estimating the financial losses due to bovine fasciolosis in Switzerland. The Veterinary Record 157(7):188-193 doi:157/7/188

Sheldrick GM (2010) Experimental phasing with SHELXC/D/E: combining chain tracing with density modification. Acta Crystallogr D Biol Crystallogr 66(Pt 4):479-85 doi:10.1107/s0907444909038360

Subpipattana P, Grams R, Vichasri-Grams S (2012) Analysis of a calcium-binding EF-hand protein family in *Fasciola gigantica*. Exp Parasitol 130:364-373 doi:10.1016/j.exppara.2012.02.005

Thomas CM, Fitzsimmons CM, Dunne DW, Timson DJ (2015) Comparative biochemical analysis of three members of the *Schistosoma mansoni* TAL family: Differences in ion and drug binding properties. Biochimie 108:40-47 doi:10.1016/j.biochi.2014.10.015 [doi]

Thomas CM, Timson DJ (2015) FhCaBP2: a *Fasciola hepatica* calcium-binding protein with EF-hand and dynein light chain domains. Parasitology:1375-1386 doi:S0031182015000736

Thomas CM, Timson DJ (2016) A mysterious family of calcium binding proteins from parasitic worms. Biochemical Society Transactions. In press.

Tina KG, Bhadra R, Srinivasan N (2007) PIC: Protein Interactions Calculator. Nucleic acids Res 35(Web Server issue):W473-6 doi:10.1093/nar/gkm423

Vichasri-Grams S, Subpipattana P, Sobhon P, Viyanant V, Grams R (2006) An analysis of the calcium-binding protein 1 of *Fasciola gigantica* with a comparison to its homologs in the phylum Platyhelminthes. Mol Biochem Parasitol 146(1):10-23 doi:S0166-6851(05)00308-7 [pii]; 10.1016/j.molbiopara.2005.10.012

Vonrhein C, Blanc E, Roversi P, Bricogne G (2007) Automated structure solution with autoSHARP. Methods in Molecular Biology 364:215-30 doi:10.1385/1-59745-266-1:215

Winkelhagen AJ, Mank T, de Vries PJ, Soetekouw R (2012) Apparent triclabendazole-resistant human *Fasciola hepatica* infection, the Netherlands. Emerg Infect Dis 18(6):1028-1029 doi:10.3201/eid1806.120302

Winn MD, et al. (2011) Overview of the CCP4 suite and current developments. Acta Crystallogr D Biol Crystallogr 67(Pt 4):235-42 doi:10.1107/s0907444910045749

Xu J, et al. (2014) *Schistosoma japonicum* tegumental protein 20.8, role in reproduction through its calcium binding ability. Parasitol Res 113(2):491-497 doi:10.1007/s00436-013-3678-7

Zhang Z, Xu H, Gan W, Zeng S, Hu X (2012) *Schistosoma japonicum* calcium-binding tegumental protein SjTP22.4 immunization confers praziquantel schistosomulumicide and antifecundity effect in mice. Vaccine 30(34):5141-5150 doi:10.1016/j.vaccine.2012.05.056

Figure legends

Fig. 1 Crystals of the dynein light chain-like domain of the *Fasciola hepatica* calcium-binding protein 2. **a** Crystal (about 0.2 x 0.15 x 0.1 mm) belonging to the $P4_12_12$ spacegroup. **b** Crystal (about 0.45 x 0.2 x 0.2 mm) belonging to the $P6_422$ spacegroup.

Fig. 2 Structure of the DLC-like domain of FhCaBP2. **a** Monomer structure. The protein chain is coloured from blue (N-terminus) to red (C-terminus) in a rainbow colour scheme. β-Strands and α-helices are labelled. **b** Dimer structure. One monomer is coloured as in the previous panel, the other in cyan. Black arrows indicate where peptide interactions take place in other DLC domains. **c** Topology diagram of the dimer. Monomers are coloured as in the previous panel.

Fig. 3 Comparison of the FhCaBP2 DLC-like domain with the modelled structure of the whole protein and with other DLC domains. **a** Superposition of the crystallographically determined structure of the FhCaBP2 DLC-like domain (in green) and the previously published model of the entire structure (in magenta). The predicted calcium ion is shown in grey and the termini of the DLC-like domain are indicated. **b** Superposition of the FhCaBP2 DLC-like domain (in green) and human dynein light chain 8 (PDB entry 3ZKE, in blue). The peptide bound to human dynein light chain 8 is shown in yellow and the $\beta_2\beta_3$-loop is highlighted with an arrow.

Table 1 Click here to download Table Table1.docx

Table 1 Crystallographic data collection, phase determination, solvent flattening and refinement statistics (all values in parenthesis are for the highest resolution bin).

Data collection	**Derivative**	**Native**
Space group	$P4_12_12$	$P6_422$
Unit cell dimensions (a, b, c) (Å)	59.9, 59.9, 81.3	57.9, 57.9, 90.0
Wavelength (Å)	1.0056	1.0047
Resolution (Å)	23.0-2.30 (2.42-2.30)	50.0-2.20 (2.32-2.20)
Observed reflections	7026 (990)	5253 (726)
Multiplicity	9.6 (9.7)	11.0 (11.7)
Completeness (%)	99.9 (100.0)	100.0 (100.0)
Rmerge (%)	11.7 (47.4)	5.7 (49.3)
<I/sigma(I)>	12.0 (4.5)	22.7 (5.0)
Wilson B (Å^2)	30.9	41.2
CC1/2	0.997 (0.929)	1.000 (0.969)
CCanom	0.567 (0.015)	-0.129 (0.049)
Phase determination		
Number of heavy atom sites (Hg)	3	-
Anomalous phasing power	1.185	-
Figure of merit (acentric / centric)	0.315/0.137	-
Solvent flattening (53.6% solvent)		
Hand score (original / inverted)	0.593 / 0.247	-
Overall correlation on $\|E\|^2$ / contrast	3.72	-
Refinement		
Resolution range (Å)	23.0-2.30 (2.36-2.30)	50.0-2.30 (2.36-2.30)
No. reflections used in refinement	6289 (445)	4093 (282)
No. reflections used for R-free	702 (44)	484 (34)
R-factor (%)	19.1 (23.0)	20.2 (29.6)
R-free (%)	24.1 (26.3)	27.5 (49.4)
Number of protein / Hg / Cl / solvent atoms	802 / 1 / 2 / 57	816 / 0 / 0 / 7
Average B protein / Hg / Cl / solvent atoms (Å^2)	37.0 / 48.4 / 62.3 / 40.4	63.1 / - / - / 55.1
Ramachandran plot (favoured / allowed) (%)	99.0 / 100.0	97.9 / 100.0
R.m.s. deviation of bonds (Å) and angles (°)	0.012 / 1.5	0.011 / 1.5
PDB code	5FWZ	5FX0

a

b

Figure 2

Click here to download Figure Fig2.tif

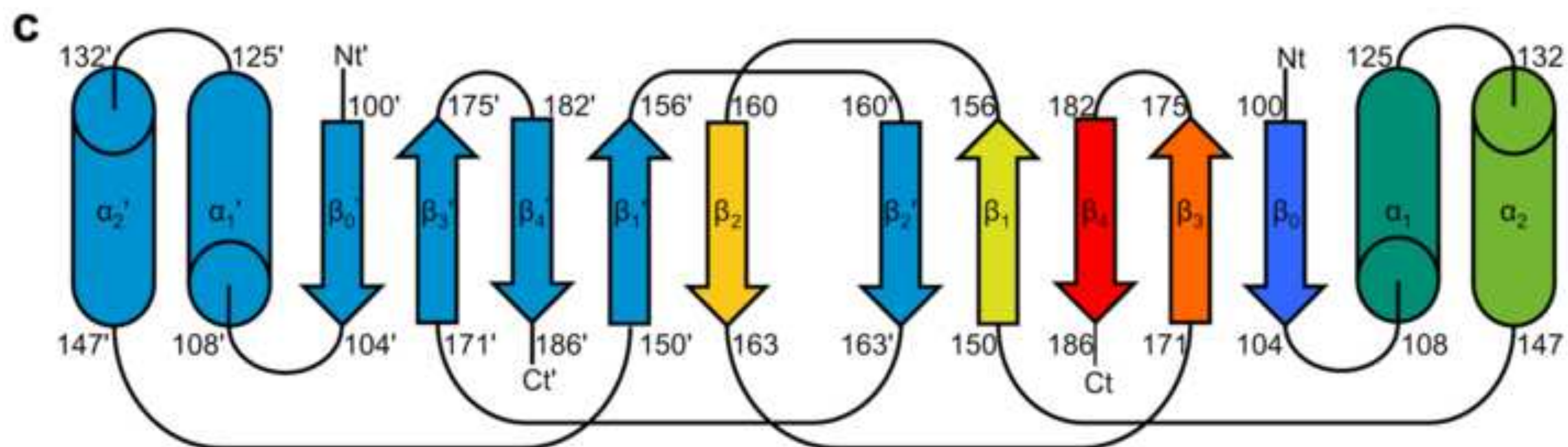

 Click here to download Figure Fig3new.tiff